

# Influence of Concentration of Vanadium in Zinc Oxide on Structural and Optical Properties with Lower Concentration \*

WANG Li-Wei(王丽伟)<sup>1,2,3</sup>, XU Zheng(徐征)<sup>1\*\*</sup>, MENG Li-Jian(孟立建)<sup>2,3</sup>, Vasco Teixeira<sup>3</sup>,  
SONG Shi-Geng(宋世庚)<sup>4</sup>, XU Xu-Rong(徐叙稼)<sup>1</sup>

<sup>1</sup>*Institute of Optoelectronics Technology, and Key Laboratory of Luminescence and Optical Information, Beijing Jiaotong University, Beijing 100044*

<sup>2</sup>*Departamento de Física, Instituto Superior de Engenharia do Porto, Rua Dr. António Bernardino de Almeida 431, 4200-072 Porto, Portugal*

<sup>3</sup>*Centro de Física, Universidade do Minho, Campus de Azurem, 4800-058 Guimarães, Portugal*

<sup>4</sup>*Thin Film Center, University of Paisley, Paisley PA1 2BE, Scotland*

(Received 19 December 2008)

ZnO films doped with different vanadium concentrations are deposited onto glass substrates by dc reactive magnetron sputtering using a zinc target doped with vanadium. The vanadium concentrations are examined by energy dispersive spectroscopy (EDS) and the charge state of vanadium in ZnO thin films is characterized by x-ray photoelectron spectroscopy. The results of x-ray diffraction (XRD) show that all the films have a wurtzite structure and grow mainly in the *c*-axis orientation. The grain size and residual stress in the deposited films are estimated by fitting the XRD results. The optical properties of the films are studied by measuring the transmittance. The optical constants (refractive index and extinction coefficient) and the film thickness are obtained by fitting the transmittance. All the results are discussed in relation with the doping of the vanadium.

PACS: 78.20. -e, 78.20. Ci, 68.55. -a

ZnO crystallizes in a hexagonal wurtzite-type structure with a band gap energy of 3.37 eV, and it could have a promising future in optoelectronics.<sup>[1–4]</sup> Research on dilute magnetic semiconductors (DMS) is motivated by their potential applications for spintronic devices that allow the control of both the spin and charge of carriers.<sup>[5]</sup> In dilute magnetic semiconductor (DMS) materials, transition or rare earth metal ions are substituted onto cation sites of the host semiconductors and are coupled with free carriers to introduce ferromagnetism.<sup>[6,7]</sup> Sato *et al.*<sup>[8,9]</sup> predicted that ZnO doped with Cr, Fe, Co, V and Ni can obtain ferromagnetism. Recently, some experimental works show that vanadium-doped ZnO can introduce ferromagnetism.<sup>[10,11]</sup> However, little work about ferromagnetism has been carried out so far. There have been some reports of ZnO:V films prepared by magnetron sputtering,<sup>[12]</sup> pulsed laser deposition,<sup>[13,14]</sup> ion plating,<sup>[15]</sup> etc. Among the deposition techniques, the magnetron sputtering technique has some advantages in comparison to the other methods.<sup>[16]</sup> This technique is quite simple and the required equipment is less expensive, and is considered to be the most favorable deposition method to obtain highly uniform films with high packing density and strong adhesion at a high deposition rate.

In this Letter, we report the influence of vanadium concentration on the structural and the optical properties of the ZnO:V thin films prepared by dc reactive

magnetron sputtering with lower concentration. It has been found that the structural and optical properties are strongly dependent on the doping concentration.

ZnO:V thin films were deposited on glass substrates by dc reactive magnetron sputtering using a zinc (99.99%) metal target with some pieces of vanadium. The distance between the target and the substrate was 50 mm. The sputtering chamber was evacuated to a base pressure below  $3 \times 10^{-3}$  Pa. During sputter deposition, the sputtering current applied to the target was fixed at 0.3 A. The substrate temperature was kept at room temperature. The sputtering gas Ar with purity 99.99% and the reactive gas O<sub>2</sub> with purity 99.99% were introduced to the chamber separately and controlled by standard mass flow controllers. The deposition pressure was 0.9 Pa at a constant oxygen partial pressure 0.3 Pa.

Vanadium concentrations in the ZnO films were detected by energy dispersive spectroscopy (EDS), and x-ray photoelectron spectroscopy (XPS) was employed to characterize the charge state of V ions in the ZnO:V films. The crystal structures of the films were characterized by XRD, using a Cu *K*α radiation source ranging from 10° to 80°. The surface morphology and cross-section microstructure of the films were observed by a scanning electron microscope (SEM). The transmittance spectra were measured from 300 nm to 2500 nm using a Shimadzu UV-3101PC spectrophotometer.

\*Supported by the National Natural Science Foundation of China under Grant Nos 60576016, 10774013, 10804006 and 10434030 (key project), the National High-Tech Research and Development Program of China under Grant No 2006AA03Z0412, the Natural Science Foundation of Beijing under Grant No 2073030, the National Basic Research Program of China under Grant No 2003CB314707, and Beijing Jiao Tong University under Grants Nos 2005SM057, 2006XM043 and 141028522.

\*\*Email: zhengxu@bjtu.edu.cn

© 2009 Chinese Physical Society and IOP Publishing Ltd

Vanadium concentrations in the ZnO films were detected by EDS measurement. It were found that the doping concentrations of the films are about 0.5, 0.9, 1.3 1.7, 2.1 mol%, respectively.

XPS was used to characterize the charge state of V ions in the ZnO:V films. Figure 1 illustrates the V 2*p* core-level photoemission spectrum from the films of concentration 2.1 mol%. Therefore, V exists in the V<sup>5+</sup> state in the ZnO:V films for this sample. The peaks near 520 eV and 522 eV are O satellite peaks.

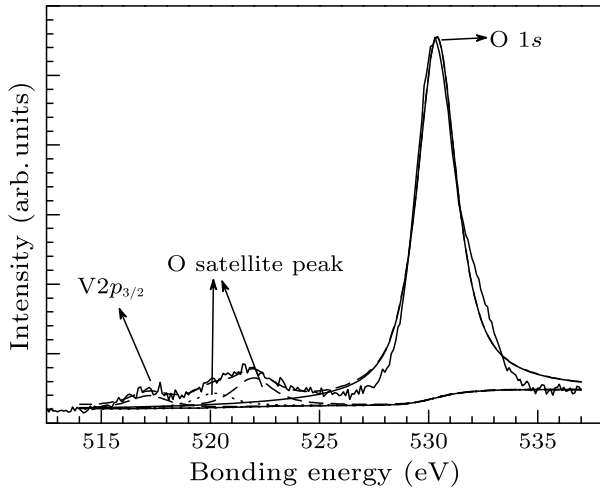


Fig. 1. XPS of the ZnO:V film with vanadium concentration 0.021 mol%.

XRD patterns of the ZnO:V films with various vanadium concentrations (0, 0.5, 0.9, 1.3, 1.7, 2.1 mol%) are shown in Fig. 2, and the ZnO:V thin films have a preferred *c*-axis orientation. No extra peaks were detected in the sensitivity of our XRD equipment. As can be seen from the XRD profile, the position of the 002 peak shifts to a smaller angle. We can estimate the parameter *c* of the films from the XRD profiles using the equation

$$2d \sin \theta = n\lambda, \quad (1)$$

where  $\lambda$  is the x-ray wavelength (Cu *K* $\alpha$  radiation  $\lambda = 1.5406 \text{ \AA}$ ), *n* is an integer, *d* is the interatomic spacing,  $c = 2d$ , and  $\theta$  is the diffraction angle. The estimated values for the films are listed in Table 1. It may be noted from Table 1 that the shifts of peak position with different vanadium concentrations are insignificant for the first three samples. With further increase of vanadium concentration, the peak position shifts to a smaller angle. The substitution in the ZnO wurtzite network should lead to a small increase of the *c*-axis lattice constant, in agreement with the variation observed in the present study for all the prepared samples.

The larger value of lattice parameter *c* indicates that the films are in a state of uniform compressive strain with strain component parallel to the *c* axis. The residual stress of the films is calculated from the value of lattice parameter of the films using the

expression<sup>[17]</sup>

$$\sigma = \frac{2c_{13}^2 - c_{33}(c_{11} + c_{12})}{2c_{13}} \frac{d - d_0}{d_0}, \quad (2)$$

where *d* is the crystallite plane spacing of the films, and  $d_0 = 2.6033 \text{ \AA}$  is the standard plane spacing from x-ray diffraction. The values of the elastic constant from single crystalline ZnO,  $c_{11} = 208.8 \text{ GPa}$ ,  $c_{33} = 213.8 \text{ GPa}$ ,  $c_{12} = 119.7 \text{ GPa}$  and  $c_{13} = 104.2 \text{ GPa}$ , are substituted in Eq. (2). The calculated residual stresses of the films are listed in Table 1. From Table 1, it can be seen that all the samples have a negative residual stress which indicates a compressive stress in the films. The residual stress of the films increases with increasing vanadium concentration. This is due to the incorporation of vanadium in ZnO.

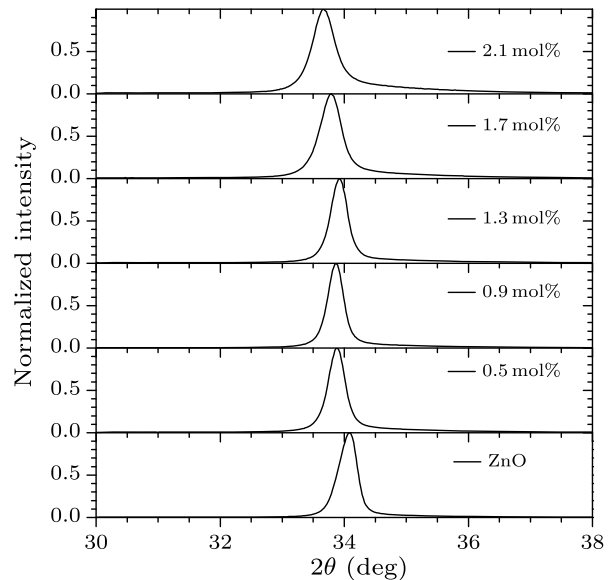


Fig. 2. XRD patterns of ZnO:V films with various vanadium concentrations.

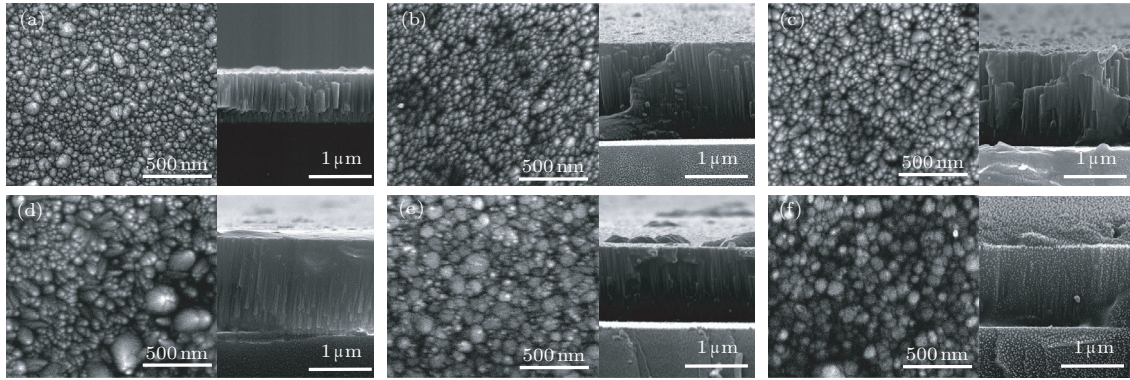
From Fig. 2, we find that the full-width at half-maximum (FWHM) of the (002) peak for vanadium concentrations of 0, 0.5, 0.9, 1.3, 1.7, 2.1 mol%, increases with increasing vanadium concentration. We use the Debye-Scherrer formula<sup>[18]</sup>

$$D = \frac{0.9\lambda}{B \cos \theta}, \quad (3)$$

where  $\lambda$  is the x-ray wavelength,  $\theta$  is the Bragg diffraction angle and *B* is the FWHM after correction for the instrument broadening. By fitting the measured x-ray diffraction data, the average crystallite size of the films has been calculated from the (002) peak. The calculated grain sizes are also listed in Table 1. The table reveals that the grain sizes decrease with increasing vanadium concentration. This may due to the fact that V ions could disturb the ZnO crystal lattice and influence the crystal growth. The phenomena are consistent with the results of Teng *et al.*<sup>[19]</sup>

Table 1. Grain size along the (001) direction, residual stress and thickness of the ZnO:V films with various V-doping concentrations.

Vanadium concentration (mol%)	$d$ (nm)	$c$ (nm)	Stress (GPa)	FWHM (deg)	Grain size (nm)	Thickness (nm)
0	0.2633	0.5266	-2.72	0.30	27.4	1506
0.5	0.2647	0.5294	-3.90	0.30	28.5	1522
0.9	0.2648	0.5296	-4.01	0.28	29.8	1433
1.3	0.2644	0.5288	-3.63	0.30	28.5	1561
1.7	0.2653	0.5306	-4.48	0.38	22.1	1231
2.1	0.2663	0.5326	-5.37	0.42	20.2	1243

**Fig. 3.** SEM micrographs of the films prepared with various vanadium concentrations: (a) ZnO, (b) 0.5 mol%, (c) 0.9 mol%, (d) 1.3 mol%, (e) 1.7 mol%, (f) 2.1 mol%.

The surface topography and cross-section morphology of the deposited ZnO:V films with various concentrations were examined by the SEM in Fig. 3. It can be seen that the average of particle size along the surface and the roughness of the films decrease with the raising of vanadium concentration, and the films have a normal columnar structure as observed from the cross section. From the side view of the cross section image, the films grow with perfect pillar-like crystal structure, which can also confirm that the film has a strong preferred orientation with the  $c$ -axis perpendicular to the substrate.

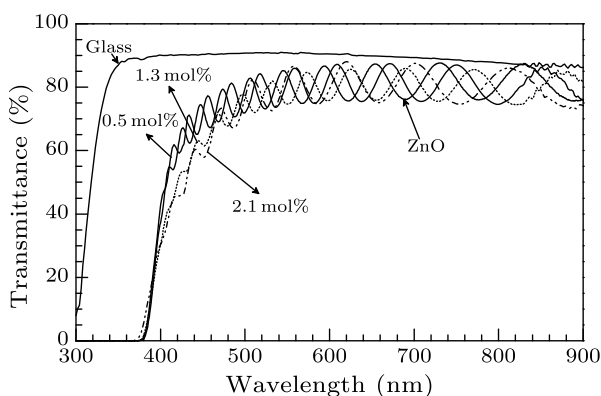
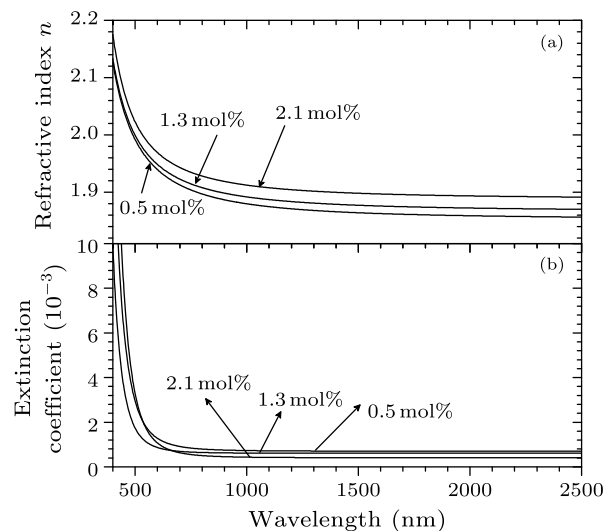
**Fig. 4.** Optical transmittance spectra of the ZnO:V films with various vanadium concentrations.

Figure 4 shows optical transmittance spectra of the ZnO:V films. The spectra of the films show wave forms (ripples), which are characteristic of the interference of light. The transmission spectra in the visible optical region are transparent, and the transmittance maxima of the films with low vanadium concentration are

higher than those of the films with higher vanadium concentration. Due to the fundamental absorption in the vicinity of the band gap, the transmittance decreases sharply as the wavelength reaches the ultra-violet range. The thickness, refractive index and extinction coefficient of films are obtained by fitting the transmittance spectra using the Drude model and the O'Leary-Johnson-Lim (OJL) model.<sup>[20,21]</sup>

The calculated refractive indices of all the ZnO:V thin films are shown in Fig. 5(a). The refractive index increases with the increase of vanadium concentration. This means that the film density increases with vanadium concentration, leading to the increase of the refractive index.

**Fig. 5.** (a) Refractive index and (b) extinction coefficient of the films with various vanadium concentrations.

The observed variation of refractive index with vanadium concentration for ZnO:V thin films can be explained on the basis of the contribution from both packing density and lattice contraction.<sup>[22]</sup> The relation of the refractive index to packing density  $p$  and lattice parameter can be expressed by<sup>[22]</sup>

$$n_f = n_f(p) + [n_f(l) - n_b] \\ = \sqrt{\frac{(1-p)n_v^4 + (1+p)n_v^2 n_b^2}{(1+p)n_v^2 + (1-p)n_b^2}} \\ + \frac{5}{2} \left( \frac{n_b^2 - 1}{2n_b d_0} \right) (d - d_0), \quad (4)$$

where  $n_f$  is the refractive index of the film,  $n_b$  is the refractive index of single crystal, and  $n_v$  is the index of the voids in the film (equal to one for air). The first and second terms in Eq. (4) represent the contribution to the refractive index from the packing density and to the changes of lattice constant  $d$ . According to Eq. (4), the refractive index of the films would increase or decrease, which depends on which it is of these two effects. In the present study, the value of  $d$  is greater than  $d_0$  for all the samples and  $n_b$  is greater than 1, therefore both the terms in Eq. (4) are positive. An increase of packing density with V content was observed and may be related to the increase of disorder and decrease of grain size with V concentration.

Figure 5(b) shows the extinction coefficient of the films with various vanadium concentrations. The extinction coefficient of the films decreases with the increase of doping concentration, in the wavelength range 600–2500 nm. However, for the concentration of 2.1 mol%, the extinction coefficient of this film increases strongly in the wavelength range 400–600 nm. This may be attributed to the V doping effect.

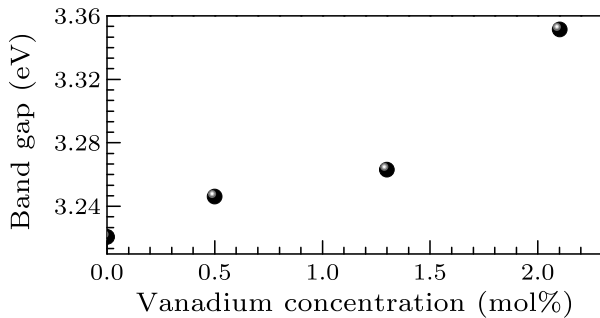


**Fig. 6.** Band gap of the films with various vanadium concentrations.

To obtain the band gap  $E_g$ , we use the relationship of the function for optical absorption and photo energy. The optical absorption coefficient of a direct band gap semiconductor near the band edge, for photon energy  $h\nu$  greater than the band gap energy  $E_g$ , is given by<sup>[23,24]</sup>

$$\alpha = A(h\nu - E_g)^{1/2}/h\nu, \quad (5)$$

$$T = (1 - R)e^{-\alpha t}, \quad (6)$$

where  $A$  is a function of the refractive index of the material, reduced mass and speed of light.  $T$  is the transmittance of the thin film,  $R$  the reflectance and  $t$  the thickness of the film obtained from the simulation. Since the reflectivity is negligible and insignificant near the absorption edge, here  $(\alpha h\nu)^2$  is a function of the energy of incident radiation. The energy band gap can be evaluated by extrapolating the linear part of the curve with the energy axis. The optical energy band gap of the films is found to increase from 3.21 to 3.35 eV with increasing doping concentration as shown in Fig. 6. These relatively high shifts may be due to grain size and the presence of impurities.

In summary, we have grown ZnO:V films with various V-doping concentrations (0, 0.5, 0.9, 1.3, 1.7, 2.1 mol%) on glass substrates using the dc reactive magnetron sputtering technique, and discussed the effect of various vanadium concentrations on the structure, morphology and optical properties of ZnO:V films in detail. From the XRD patterns of ZnO:V films, the samples have a preferential  $c$ -axis orientation, and the grain size along the (001) direction decreases as the vanadium concentration increases. The SEM images show the surface topography and cross-section morphology of the deposited ZnO:V films, which indicates that the films have good crystallinity and texture. The transmittance spectra of all the films show good optical quality. Refractive indices and extinction coefficients of the films are obtained by fitting from the transmittance spectra using the Drude model and the OJL model.

## References

- [1] Özgür Ü et al 2005 *J. Appl. Phys.* **98** 041301
- [2] Zhang X Y et al 2007 *Chin. Phys. Lett.* **24** 1032
- [3] Lin Q G et al 2008 *Chin. Phys. Lett.* **25** 4223
- [4] Yang P D et al 2002 *Adv. Funct. Mater.* **12** 323
- [5] Ohno H 1998 *Science* **281** 951.
- [6] Dietl T et al 2000 *Science* **287** 1019
- [7] Pearton S J et al 2004 *J. Vac. Sci. Technol. B* **22** 932
- [8] Sato K et al 2000 *Jpn. J. Appl. Phys. II* **39** L555
- [9] Sato K and Katayama-Yoshida H 2001 *Physica E* **10** 251
- [10] Zhang F C et al 2009 *Chin. Phys. Lett.* **26** 016105
- [11] Sato K et al 2001 *Jpn. J. Appl. Phys. II* **40** L334
- [12] Ruan Y B et al 2006 *Chin. J. Inorg. Chem.* **22** 2247
- [13] Ishida Y et al 2004 *Physica B* **351** 304
- [14] Hong N H et al 2005 *J. Appl. Phys.* **97** 312
- [15] Vyatkin A F et al 2005 *Nucl. Instrum. Method. Phys. Res. B* **237** 179
- [16] Ye Z Z and Tang J F 1989 *Appl. Opt.* **28** 2817
- [17] Wang Y G et al 2003 *J. Appl. Phys.* **94** 1597
- [18] Weller M T 1997 *Inorganic Materials Chemistry* (Oxford: Oxford University)
- [19] Teng X Y et al 2007 *Chin. Phys. Lett.* **24** 1073
- [20] Solieman A et al 2006 *Thin Solid Films* **502** 205
- [21] O'Leary S K, Johnson S R and Lim P K 1997 *J. Appl. Phys.* **82** 3334
- [22] Mehan N et al 2004 *J. Appl. Phys.* **96** 3134
- [23] Hong W Q 1989 *J. Phys. D* **22** 1384
- [24] Berggren L et al 2001 *J. Appl. Phys.* **90** 1860